Trends in the deep Southern Ocean (1958–2010): Implications for Antarctic Bottom Water properties and volume export

ARTICLE *in* JOURNAL OF GEOPHYSICAL RESEARCH ATMOSPHERES · SEPTEMBER 2013

Impact Factor: 3.43 · DOI: 10.1002/jgrc.20303

4 AUTHORS:

Marina Azaneu
University of East Anglia
7 PUBLICATIONS **14** CITATIONS
SEE PROFILE

Rodrigo Kerr
Universidade Federal do Rio Grande (FURG)
26 PUBLICATIONS **67** CITATIONS
SEE PROFILE

Mauricio M. Mata
Universidade Federal do Rio Grande (FURG)
71 PUBLICATIONS **500** CITATIONS
SEE PROFILE

Carlos A. E. Garcia
Universidade Federal do Rio Grande (FURG)
77 PUBLICATIONS **874** CITATIONS
SEE PROFILE

Trends in the deep Southern Ocean (1958–2010): Implications for Antarctic Bottom Water properties and volume export

Marina Azaneu,[1] Rodrigo Kerr,[1] Mauricio M. Mata,[1] and Carlos A. E. Garcia[1]

Received 4 January 2013; revised 24 June 2013; accepted 3 July 2013.

[1] Regional formation of deep and bottom water masses around the Antarctic continental shelf is one of the most important processes contributing to variability of the global meridional overturning circulation deep cell. Southern Ocean hydrographic data collected during the years 1958–2010 indicate that dense shelf waters cooled and freshened during that period. In the surrounding open ocean, Antarctic Bottom Water (AABW) warmed, with no evidence of salinity change. As a result of source-water property changes, AABW exported from the Southern Ocean to the deep world ocean became lighter over the period analyzed. The average rate of density change within the areas that experienced statistically significant change was -0.0019 kg m^{-3} yr^{-1}. For the last 20 years of the analysis, a negative AABW volume anomaly (relative to the half-century average, 1958–2010) was indicated, possibly due to production of a lighter AABW variety or to changes in formation rates. Over the entire five decades, the upper isopycnal of the AABW layer deepened at a rate of -8.1 m yr^{-1}. Changes in fundamental hydrographic properties such as these can have important implications for long-term global ocean circulation and climate.

Citation: Azaneu, M., R. Kerr, M. M. Mata, and C. A. E. Garcia (2013), Trends in the deep Southern Ocean (1958–2010): Implications for Antarctic Bottom Water properties and volume export, *J. Geophys. Res. Oceans*, *118*, doi:10.1002/jgrc.20303.

1. Introduction

[2] Understanding Southern Ocean processes is important in developing a refined understanding of recent changes in global climate. This circumpolar ocean serves as the main ventilation area for deep and bottom layers of the world ocean [*Broecker et al.*, 1998] and is a major player in global heat and freshwater transport [*Schmittner et al.*, 2007]. It is also one of the world's most biologically productive regions [*Mayewski et al.*, 2009] and serves as a significant sink for anthropogenic carbon dioxide [*Orsi et al.*, 1999].

[3] Antarctic Bottom Water (AABW), one of the densest waters in the global ocean, covers the majority of the world ocean floor. Its formation occurs in specific regions around the Antarctic margin, with contributions from several different source water masses [*Carmack and Foster*, 1975]. The main mechanism for dense water formation involves surface forcing—e.g., source water cooling due to heat loss, and salinity increase due to sea ice formation and brine rejection—in addition to mixing with surrounding waters during downslope flow [*Foster and Carmack*, 1976]. The process of dense water mass formation significantly influences the global meridional overturning circulation (MOC) deep cell [*Lumpkin and Speer*, 2007]. The MOC transports a large amount of water, heat, salt, carbon, nutrients, and other substances around the world, thus strongly influencing global and regional climatic patterns [*Schmittner et al.*, 2007].

[4] Several studies have documented significant recent changes in regional climate around the Antarctic continent—for example, atmospheric warming [*Turner et al.*, 2005] and glacial retreat in the Antarctic Peninsula region [*Cook and Vaughan*, 2010]. In 2002 the Larsen B ice shelf collapsed in association with rising summer air temperatures [*Rignot et al.*, 2004] and basal melt [*Pritchard et al.*, 2012] linked to changes in wind forcing [*Marshall et al.*, 2006]. Intense warming (+1°C) and increasing salinity (+0.25) have also been reported for surface waters of the western Antarctic Peninsula [1955–1998; *Meredith and King*, 2005].

[5] Recent changes have not been confined to terrestrial and surface-ocean environs; intermediate and deep waters are changing as well. A significant temperature increase (+0.2°C during the 1990s) was observed in intermediate-depth waters of the Antarctic Circumpolar Current [*Gille*, 2002] as well as in Warm Deep Water (WDW) within the Weddell Gyre (+0.012°C yr^{-1}, 1970s–1990s) [*Robertson et al.*, 2002]. Waters below 4000 dbar within the Weddell-Enderby Basin, the Australian-Antarctic Basin, and the Southeast Pacific Basin all warmed (+0.33, +0.24, and +0.15 W m^{-2}, respectively, for the 1990s–2000s) [*Purkey and Johnson*, 2010]. Within the inner Weddell Sea, Weddell Sea Bottom Water (WSBW) also warmed (+0.01°C yr^{-1}, 1989–1995). In the region of the prime meridian, temperature

[1]Laboratório de Estudos dos Oceanos e Clima, Instituto de Oceanografia, Universidade Federal do Rio Grande, Rio Grande, Brazil.

Corresponding author: M. Azaneu, Laboratório de Estudos dos Oceanos e Clima, Instituto de Oceanografia, Universidade Federal do Rio Grande, Rio Grande, RS 96203-900, Brazil. (m.azaneu@furg.br)

2169-9275/13/10.1002/jgrc.20303

increase (+0.003°C yr^{-1}) with no countering change in salinity led to less dense WSBW during the second half of the 1990s [*Fahrbach et al*., 2004]. A longer-term study in the same region documented decreasing temperature and salinity in Weddell Sea Deep and Bottom Water (1984–1992), followed by increasing temperature and salinity (1998–2008) [*Fahrbach et al*., 2011]. Rapid AABW freshening occurred in the Indian and Pacific sectors of the Southern Ocean during 1995–2005 [*Rintoul*, 2007]. Freshening has also been reported for high-latitude deep waters of the south Pacific and Atlantic Oceans for the period between the late 1950s and the mid-1990s [*Boyer et al*., 2005]. Adelie Land Bottom Water along 140°E experienced temperature and salinity decreases from 1994 to 2002 (−0.2°C temperature change and −0.03 salinity change) [*Aoki et al*., 2005]. Warming and freshening have been reported for abyssal waters at Princess Elizabeth Trough (+0.05°C and −0.01) and in the Australian-Antarctic Basin (+0.1°C and −0.005) between 1994/1995 and 2007 [*Johnson et al*., 2008].

[6] In several shelf regions, recent salinity reductions have been noted—e.g., the northwestern Weddell Sea [*Hellmer et al*., 2011], George V continental shelf and rise (140°–150°E), and Ross Sea [*Jacobs et al*., 2002; *Jacobs and Giulivi*, 2010; *Jacobs*, 2004]. Salinity changes are very important in the Southern Ocean due to the nonlinearity of the equation of state of seawater [*Fofonoff*, 1956]. At low temperatures, salinity is the main determinant of seawater density, thereby exerting great influence on water column stratification and geostrophic flow [*Mayewski et al*., 2009].

[7] The many recent, complex changes in the Antarctic ocean-atmosphere-cryosphere system are yet poorly understood but may have important global implications. For example, a possible weakening in the production and advection of North Atlantic Deep Water and AABW could have substantial consequences for marine ecosystems, global sea level, and the intertropical convergence zone and its associated tropical rainfall belts [e.g., *Rahmstorf*, 2006].

[8] In this work, we report on the use of an extensive observational data set to examine spatial and temporal variability in hydrographic properties of Southern Ocean dense water masses in all Antarctic marginal seas (shelf and open ocean) for the period of 1958–2010. We also determined decadal AABW layer thickness and changes in AABW volume. Section 2 describes the database and methodology. Section 3 presents hydrographic property trends and discusses them in the context of other observations. AABW volume anomalies and processes that might be driving the observed changes are also considered. Section 4 recaps major findings and discusses their implications.

2. Database and Methodology

2.1. Hydrographic Data Sets, 1958–2010

[9] The data set used here is derived from three sources: (1) World Ocean Database 2009 [WOD09, *Boyer et al*., 2009], which consists of bottle, profiling float, and conductivity-temperature-pressure (CTD) data, 1958–2010; (2) Alfred Wegener Institute CTD data, 2003–2010; and (3) Brazilian High Latitude Oceanography Group (GOAL; www.goal.furg.br) CTD data, 2003–2005 [e.g., *Garcia and Mata*, 2005] and 2008–2010 [e.g., *Mendes et al*., 2012]. The WOD09 database includes only those measurements considered to be of good quality, as defined by the WOD quality flag [*Johnson et al*., 2009]. The combined data sets cover waters south of 60°S over a period of 53 years (1958–2010). We restricted our analysis to austral summer (November to March) because of seasonal variability and a lack of observations during other seasons.

[10] Ocean measurement techniques and accuracies changed over the half-century analyzed. The earliest data are primarily from bottle samples and low-resolution CTD records. Later data are from higher-quality CTDs (beginning in the 1960s) and free-floating profiling floats (beginning in the 1990s with PALACE and, more recently, Argo). The later PALACE floats carried sensors with accuracies of 0.002°C in temperature and 0.005 in salinity [*Boyer et al*., 2009]. The GOAL measurements had accuracies of approximately 0.002°C for temperature and 0.003 for salinity, for all cruises. The accuracy of the CTD data within the combined data set ranges from 0.001 to 0.005°C for temperature and approximately 0.003 to 0.02 for salinity (PSS).

[11] Three hydrographic parameters are analyzed in this work: potential temperature θ, salinity S, and neutral density γ^n [*Jackett and McDougall*, 1997]. Our analysis focuses on waters of $\gamma^n \geq 28.27$ kg m^{-3} (i.e., dense waters), which includes dense shelf waters [e.g., *Nicholls et al*., 2009; *Orsi and Wiederwohl*, 2009] and all the several varieties of AABW produced around the continental margins [e.g., *Whitworth et al*., 1998] and exported to the global ocean (as described by *Orsi et al*. [1999]). This density-based definition of dense water was recently applied in a model-based investigation of AABW production and export [*Kerr et al*., 2012].

[12] The data set was divided into "shelf" (dense shelf waters) and "open ocean" (AABW layer) hydrographic regimes, with the 1300 m isobath defining the boundary between the two (Figure 1a). An exception was made for the bottom water masses of the Bransfield Strait deep basins. Despite their great depth, these waters are included in the shelf regime because their major source waters, which originate on the Weddell Sea northwestern continental shelf, take a brief, direct route to the strait's deep basins [*Whitworth et al*., 1994].

[13] The data set was further divided into five regional hydrographic sectors according to the zones defined by *Cavalieri and Parkinson* [2008]: the Bellingshausen/Amundsen Sea, Ross Sea, Western Pacific, Indian, and Weddell Sea sectors (Figure 1a). The regions sampled most frequently during the half-century under consideration are (i) the continental shelves of the Ross Sea and Prydz Bay, (ii) the Bransfield Strait zone, and (iii) the open ocean regions of the Weddell Sea, Indian, and Western Pacific sectors (Figure 1b). Data coverage in the Bellingshausen/Amundsen Sea and western Ross Sea sectors is particularly sparse. Some stations were sampled more deeply than others, but because ~75% of our profiles extend to within 500 m of the sea bottom (i.e., to a depth where the bottom waters are relatively homogeneous vertically), we assume that our results are not biased by differences in maximum sampling depth.

[14] Two approaches were adopted for the construction of annual time series of hydrographic properties: (1) an examination of time-varying local anomalies for the whole

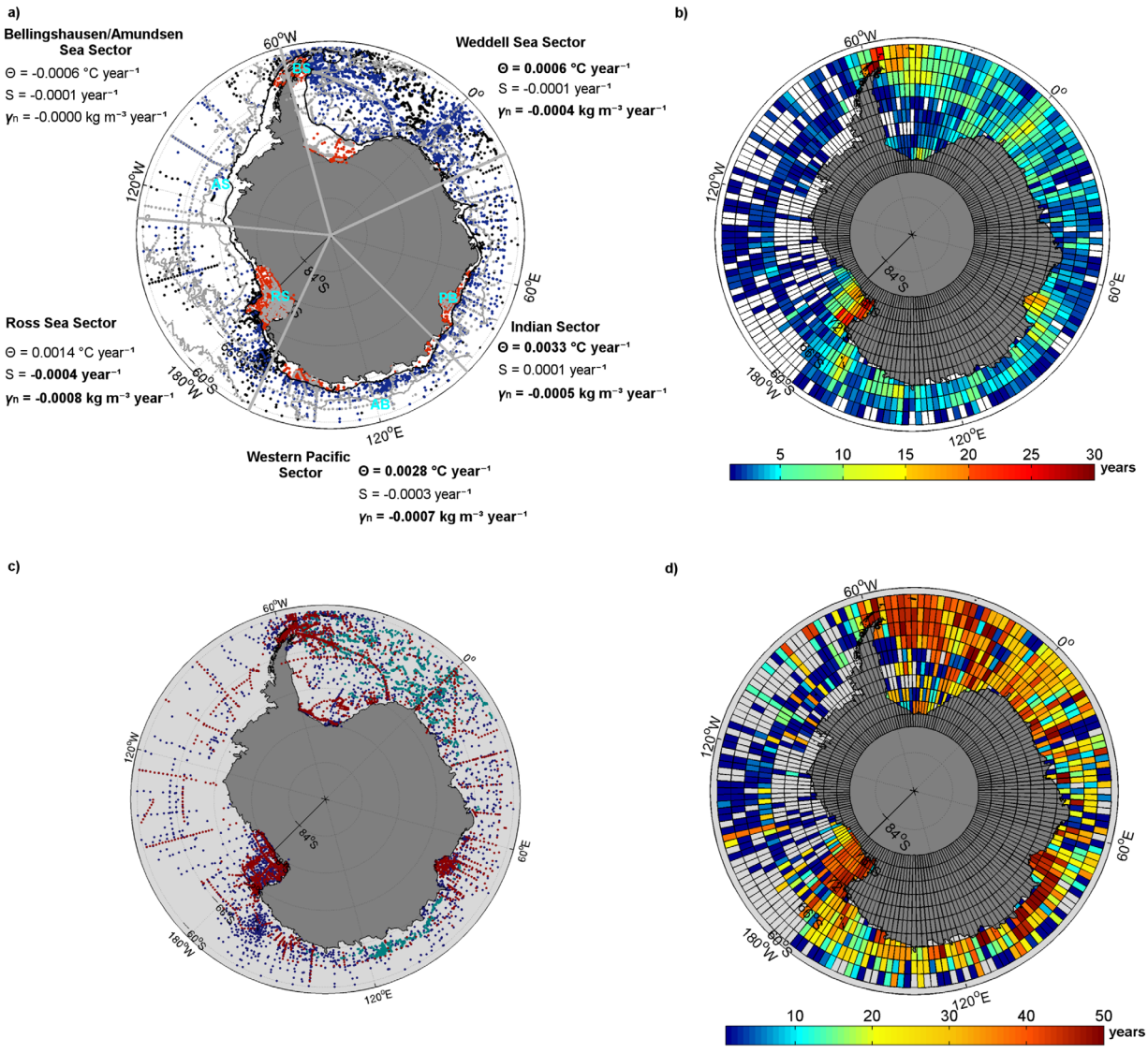

Figure 1. Observations of potential temperature θ, salinity S, and neutral density γ^n in Southern Ocean dense water masses, 1958–2010. (a) Gray dots show the locations of measurements made during the 1990–2000 reference decade. Colored dots represent station locations within 222 km of a reference station: red for shelf data and blue for open ocean data. The black dots show data points excluded from the calculation of local anomalies but included in the calculation of time trends within individual grid cells. The black and gray contour lines indicate the 1300 and 4000 m isobaths, respectively. The radiating gray boundary lines delineate hydrographic sectors. Temporal trends of local hydrographic anomalies in the open ocean waters of each sector are also given, with bold numbers indicating statistically significant trends (DBIN approach). The locations of the Bransfield Strait (BS), Amundsen Sea (AS), Ross Sea shelf (RS), Prydz Bay (PB), and Australian-Antarctic Basin (AB) regions are indicated. (b) The number of distinct years sampled within each 2° grid cell. (c) Data types: blue indicates bottle data; green indicates profiling float data, and red indicates CTD data. (d) Number of years between the earliest and latest measurements within each grid cell.

Southern Ocean and its individual regional sectors and (2) an examination of time-varying absolute property values within 2° grid cells (subsequently averaged to give whole-ocean and regional mean trends).

2.2. Calculation of Circum-Antarctic and Regional Hydrographic Anomaly Trends

[15] The water layer below the 28.27 kg m^{-3} isopycnal is not homogenous across the Southern Ocean basins. In addition, the spatial distribution of hydrographic data from this layer varied from year to year within our data set. Under these conditions, using absolute property values to calculate large-scale (whole-ocean or regional) time-series trends could have produced biased results. Therefore, local property anomalies were used instead. We defined anomalies relative to the years 1990–2000 because of this decade's extensive data coverage, including high-quality World Ocean Circulation Experiment (WOCE) data.

[16] We first selected for hydrographic stations located within 222 km (approximately two latitude degrees) of an observation made during the reference decade (1990–2000). We assumed that stations were randomly distributed within the selection circles—i.e., that differences in station distributions within these areas were not a source of systematic error. Application of this radius-based selection criterion excluded all open ocean data obtained in 1962. The distribution of the remaining data is shown in Figure 1a.

[17] For each station profile paired with a nearby 1990s reference profile, each hydrographic parameter was averaged within 200 m depth strata (bins). The difference between each stratum average relative to its paired 1990s stratum average was then calculated. Finally, all stratum differences were averaged vertically to produce a single average difference (anomaly) value for that parameter pair at that station location. Stations that fell within 222 km of multiple reference stations were used within multiple pairings. Reference stations were not assigned any anomaly value. Filling years from the 1990s reference decade with values of zero could have strongly influenced the calculation of the time series trends and generated misleading interpretations.

[18] We compared three different methods of areally (geographically) averaging each year's station anomalies. In the first, the "NOBIN" approach, we simply averaged, by year, all station anomaly values within the area of interest (i.e., the circum-Antarctic Southern Ocean or a regional sector). Half-century time series were then constructed from the annual (summer) mean θ, S, and γ^n anomaly values. Finally, linear fits, confidence bounds for the estimated trends, and statistical p values (considering 95% confidence levels) were determined for each time series. With this NOBIN method, every observation is weighted equally in the annual averages, and the results are therefore most representative of well-sampled areas.

[19] The other two approaches incorporated spatial binning before areal averaging: the Southern Ocean was divided into 2° grid cells (Figure 1b) and average annual (summer) anomalies were calculated within each cell. If a cell straddled the 1300 m isobath (the boundary between our shelf and open ocean regimes), only the open ocean data were used. The two cell-based approaches differed in their handling of empty cells. In the "DBIN" method, empty cells were simply excluded from the calculation of annual areal averages. In the "MBIN" method, an annual areal average was first calculated for each regional Southern ocean sector (Figure 1a) based only on cells that contained anomaly values (as with the DBIN approach). The mean value obtained for each ocean sector was further assigned to all empty cells within the respective sector, and then the annual areal average for the area of interest was calculated. Finally, as with the NOBIN approach, half-century time series were constructed from the DBIN and MBIN annual anomalies, and linear fits, confidence bounds for the estimated trends, and statistical p values were determined.

2.3. Calculation of Local and Regional Hydrographic Property Trends

[20] Temporal trends within the individual 2° grid cells (Figure 1) were also examined. For this analysis, absolute property values (rather than anomalies) could be used because the data were being evaluated locally and were therefore not influenced (biased) by horizontal differences in hydrographic properties or temporal differences in data coverage across the domain. To ensure adequate temporal coverage within each cell, we used only those cells containing data that (a) covered at least 3 distinct years (Figure 1b) and (b) spanned 10 or more years between the earliest and latest measurements (Figure 1d). Of the original 647 grid cells that contained some data, 65% met these selection criteria.

[21] To calculate regional time series trends, we further filtered the data set to include only those grid cells that exhibited a statistically significant temporal trend according to linear regression. Regional rates of change were then computed by averaging over all grid-cell trend values within the region. Confidence bounds were determined as a measure of uncertainty.

2.4. Calculation of AABW Volume Changes

[22] To investigate AABW volume changes, the open ocean data were grouped into five decadal bins. For each decade, the top of the AABW layer was taken to be the surface defined by a polynomial fit of the shallowest occurrences of $\gamma^n \geq 28.27$ kg m^{-3} in the vertical data profiles. The bottom of the layer was taken to be the seabed. Bathymetric data were obtained from the ETOPO2v2 Global Gridded 2 min database (U.S. National Geophysical Data Center, http://www.ngdc.noaa.gov/mgg/global/etopo2.html). The fitted surface was extracted to a 0.5° grid, and decadal AABW volume was then calculated as the integral from the gridded upper surface to the seabed. Due to the existence of large poorly sampled areas (e.g., the Bellingshausen/Amundsen Sea and western Ross Sea sectors), a quality mask was used to exclude areas where the data density was too low for robust spatial interpolation. Any interpolated point more than 333 km (approximately 3° of latitude) from a real (i.e., directly measured) data point was omitted.

3. Trends in Hydrographic Properties of Dense Southern Ocean Water Masses

3.1. Circum-Antarctic Anomaly Trends: Shelf and Open Ocean

[23] Time series of average annual hydrographic property anomalies of dense water masses (i.e., shelf and open ocean layers of $\gamma^n \geq 28.27$ kg m^{-3}), 1958–2010, are presented in Figure 2. Linear fits (slopes) and confidence bounds (95% confidence level) are given in Table 1. For the shelf regime (Figure 2a and Table 1), no statistically significant linear trends were indicated for potential temperature (for any geographic binning scheme). Statistically significant decreasing trends were obtained for salinity and neutral density (for all binning schemes). It seems that shelf freshening, in the absence of a counterbalancing temperature decrease, led to a decline in the neutral density of Antarctic dense shelf waters over the period examined.

[24] For the open ocean regime (Figure 2b and Table 1), a warming trend was obtained in all approaches, statistically significant considering the two bin-based methods only. No significant salinity change was indicated (by any

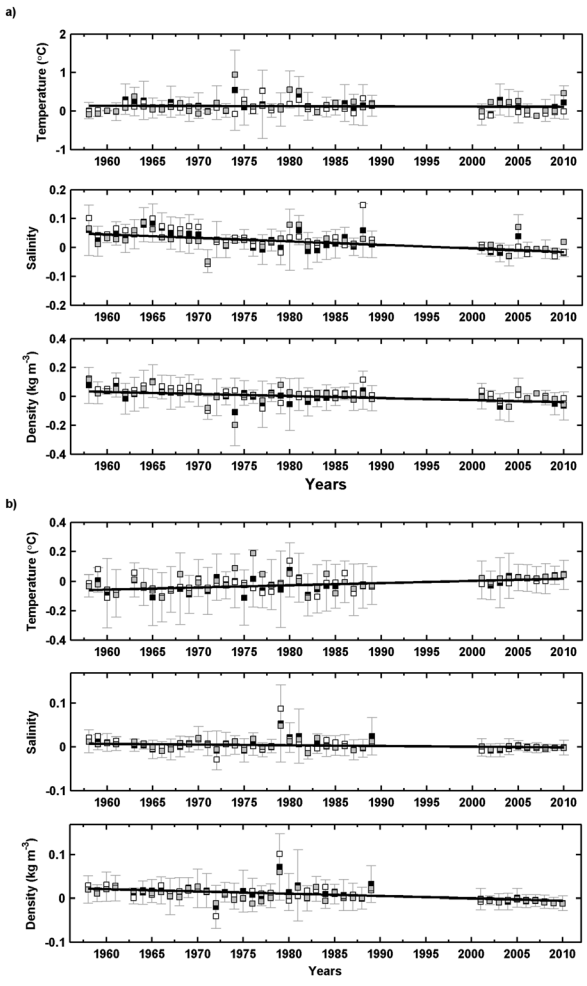

Figure 2. Annual average values of local anomalies (relative to 1990–2000 values) of potential temperature, salinity, and neutral density for Southern Ocean dense water masses, calculated using three geographic binning methods: NOBIN (open squares), DBIN (black-filled squares), and MBIN (gray-filled squares). The vertical gray bars show the standard deviations of the DBIN annual averages; the black lines show linear fits of the DBIN averages. Trends and confidence bounds for all three binning methods are given in Table 1. (a) Shelf regime and (b) open ocean regime.

method). The combined result of the potential temperature and salinity trends was a statistically significant decrease in neutral density (for all three binning methods).

[25] Thus, for both shelf and open ocean waters, density decreased over the period of study. On the shelf as a whole, freshening was the driving force. In the open ocean, warming was the major driver.

[26] Assuming that the calculated annual rates of anomaly change (Table 1) were constant for the whole 50 year period analyzed, the total amount of change of θ, S, and γ^n was greater than the instrumental accuracy. Moreover, for global zonally averaged salinity, a rate of change greater than ± 0.0005 yr^{-1} is considered to be a significant trend [*Boyer et al*., 2005]. Our estimated rates of salinity change for the shelf regime were greater than this threshold; but open ocean (AABW) regime change rates were not. This assessment of significance agrees with the statistical significance assessed by the p value, which indicates robustness for shelf-regime freshening only.

3.1.1. Effects of Geographic Binning Scheme

[27] Table 1 and Figure 2 show that the time series produced by the different binning approaches were quite similar. However, the linear fits of the shelf data (Figure 2a and Table 1) were more sensitive to choice of binning scheme than were the open ocean fits (Figure 2b and Table 1).

[28] Decreasing the influence of intensively sampled shelf areas (i.e., using the DBIN method) rather than equally weighting all measurements (the NOBIN method) resulted in different annual averages and in linear fits that indicated less change over time. The MBIN approach decreased the trends, and its statistical significance, of the shelf S and γ^n time series and maintained the general negative pattern of temporal variability. The MBIN shelf temperature trend, however, was intermediate in magnitude and opposite in sign. The MBIN assumption that empty (no-data) cells experienced changes similar to their regional averages seemed to affect the shelf trends.

[29] For the open ocean regime (Figure 2b), the different binning methods produced different annual averages (mostly in years that presented high standard deviations) but rather similar temporal trends. The DBIN approach resulted in the smallest variance of annual averages and standard deviations. These lower variances indicate more homogeneity of the time series and likely contribute to the greater statistical significance of the DBIN open ocean θ trends. Differently than in shelf waters, the MBIN approach decreased the trend and the statistical significance of the open ocean temperature time series but maintained the general pattern of temporal variability. The sampled areas within the shelf regime were regionally restricted and the proportion of empty cells thus filled by the MBIN methodology was greater than the open ocean area. This data paucity possibly contributes to disguising local or subtle trends, e.g., a shelf cooling trend, when the total time series is determined.

[30] In an earlier work, the choice of a geographic binning method was found to significantly influence the heat content change calculated for the Southern Hemisphere ocean (1950s–2000s) [*Gille*, 2008]. A substantial warming of the ocean's upper 700 m was indicated, but estimates of the increase in heat content varied from 4.3×10^{22} J to 20×10^{22} J (summer-only data), depending on the choice of a binning method. The assumption of zero temporal change for all no-data bins (5° by 5°) produced the smallest trend estimates, while pooling all data (no geographic bins) produced the largest estimates. Other binning methods produced intermediate values. Similarly, our shelf regime presented the largest trends when no geographic averaging was applied (Figure 2a and Table 1; for all hydrographic properties). However, the influence of binning method was not as strongly evident in our results as in those of *Gille* [2008]. There, the greater sensitivity to binning method may be due to the larger and more diverse region of study.

[31] In most cases, our DBIN method produced intermediate trend values compared to estimates returned by the other two methods. DBIN trends were less strongly influenced than NOBIN trends by data from the most heavily

Table 1. Linear Fits and Confidence Bounds (95% Confidence) of Annual Time Series of Local Hydrographic Anomalies, 1958–2010[a]

Hydrographic Property	Method	Trend in yr^{-1} (Confidence Bounds) Shelf Regime	Open Ocean Regime
Temperature θ (°C)	NOBIN	−0.0023 (±0.0003)	0.0010 (±0.0009)
	DBIN	−0.0005 (±0.0007)	**0.0015** (±0.0007)
	MBIN	0.0013 (±0.0008)	**0.0012** (±0.0009)
Salinity S	NOBIN	**−0.0016** (±0.0003)	−0.0003 (±0.0003)
	DBIN	**−0.0012** (±0.0007)	−0.0002 (±0.0002)
	MBIN	**−0.0008** (±0.0008)	−0.0002 (±0.0002)
Density γ^n ($kg\ m^{-3}$)	NOBIN	**−0.0015** (±0.0005)	**−0.0005** (±0.0003)
	DBIN	**−0.0014** (±0.0007)	**−0.0005** (±0.0002)
	MBIN	**−0.0011** (±0.0008)	**−0.0005** (±0.0002)

[a]Bold values indicates a statistically significant trend ($p \leq 0.05$).

sampled areas, and the DBIN method did not strongly attenuate subtle trends as did the MBIN approach. Therefore, we consider the DBIN spatial binning approach to be the most appropriate among those assessed. Our discussion of circum-Antarctic and regional (sector) anomaly trends (e.g., section 3.2) will hereafter focus on the DBIN estimates.

[32] We conducted additional sensitivity tests (results not shown), including (i) calculation of Southern Ocean time series using weighted averages based on the area occupied by each cell; (ii) sorting of shelf water data into smaller geographic bins (1° grid cells), and (iii) ignoring data within the regime boundary region (i.e., between the 800 and 1500 m isolines). None of these methodological variations strongly affected the results, indicating that the results reported above are robust.

3.2. Regional (Sector) Anomaly Trends

[33] Hydrographic property anomaly trends were also assessed for each geographic sector shown in Figure 1a. The annual time series from the five shelf areas indicated, with a single exception, no statistically significant region-specific changes in θ, S, or γ^n (results not shown).The only exception is the Ross Sea, where significant freshening was indicated ($\Delta S = -0.0004\ yr^{-1}$). The apparent lack of temporal change within individual shelf regions is probably due to the general paucity of shelf data (Figure 1a).

[34] Among the five open ocean regions, three exhibited statistically significant warming trends (Figure 1a). The highest rates of θ increase occurred in the Indian and Western Pacific sectors, followed distantly by the Weddell Sea sector. The trends indicated for the other two sectors (Bellingshausen/Amundsen Sea cooling and Ross Sea warming) were not statistically significant. For salinity, the open ocean pattern was the same as that of shelf waters: only the Ross Sea sector presented a statistically significant trend (freshening, with $\Delta S = -0.0004\ yr^{-1}$). For neutral density ($\gamma^n$), four sectors exhibited a statistically significant negative trend, with the greatest decrease seen in the Ross Sea and the least in the Weddell Sea. No statistically significant trend was indicated for the data-poor Bellingshausen/Amundsen Sea sector. The different sector-specific rates of change are probably due to different physical processes operating within the various regions.

3.3. Property Trends Within Individual Grid Cells

[35] Temporal trends of hydrographic properties within each 2° grid cell are presented in Figures 3–5. Figures 3a, 4a, and 5a show results for all grid cells, regardless of statistical significance. For all shelf areas sampled around the Antarctic continent, cooling trends were indicated (Figure 3a). Most shelf waters also showed decreasing salinity (Figure 4a) and decreasing density (Figure 5a). For the open ocean regime (i.e., AABW), warming was clearly evident in most of the sampled cells (Figure 3a). Salinity trends, in contrast, showed no clear pattern (Figure 4a). Decreasing AABW density was generally indicated over the entire Southern Ocean (Figure 5a).

[36] Figures 3b, 4b, and 5b show the locations of grid cells with statistically significant annual time trends. Among all the cells for which θ trends were calculated (Figure 3a), ~15% exhibited statistical significance (Figure 3b). For S, the proportion was ~13% (Figures 4a and 4b), and for γ^n, the proportion was ~21% (Figures 5a and 5b). These cells covered approximately 10–15% of the total Southern Ocean area (9% for θ, 8% for S, and 14% for γ^n).

[37] Figures 3c, 4c, and 5c show the statistically significant time series from the shelf regime. The trends were grouped according to location (as shown by the colors in the Figures 3b, 4b, 5b and 3c, 4c, 5c), and an average time trend was then computed for each group. Cooling trends were observed in the well-sampled shelf areas: the Ross Sea ($\Delta\theta = -0.0053 \pm 0.0017$°C yr^{-1}), the Bransfield Strait and waters just west of the Antarctic Peninsula ($\Delta\theta = -0.0278 \pm 0.085$°C yr^{-1}), the southeastern Weddell Sea ($\Delta\theta = -0.0183 \pm 0.1366$°C yr^{-1}), and Prydz Bay ($\Delta\theta = -0.0039 \pm 0.0193$°C yr^{-1}). Data from the Bransfield-western Antarctic Peninsula group exhibited the generally highest θ values and the greatest net θ decline over the period of observation. The one grid cell just west of the peninsula presented notably high annual means and a steep cooling trend. When this series was excluded from the trend calculation, a cooling rate of $\Delta\theta = -0.0081 \pm 0.0174$°C yr^{-1} was obtained for the Bransfield Strait region, more in line with the rates of change seen in the other shelf areas. The mean temperature trend determined for the entire shelf regime was -0.011 ± 0.0087°C yr^{-1}. Exclusion of the one grid cell just west of the Antarctic Peninsula yielded a shelf-regime rate of -0.0072 ± 0.0036°C yr^{-1}.

[38] Freshening was also seen on the shelves (Figure 4c). The Ross Sea, which was the saltiest, exhibited the strongest salinity decrease ($\Delta S = -0.0022 \pm 0.0007\ yr^{-1}$). Salinity decreased more slowly in the Bransfield Strait ($\Delta S = -0.0012 \pm 0.002\ yr^{-1}$), the southeastern Weddell Sea ($\Delta S = -0.0013 \pm \text{inf}\ yr^{-1}$), and Prydz Bay ($\Delta S = -0.0014 \pm \text{inf}\ yr^{-1}$). (In regions where trend values were determined from a single grid point, confidence bounds are not applicable. Such cases are indicated by "± inf"). The mean rate of salinity change for the entire shelf regime was $-0.002 \pm 0.0006\ yr^{-1}$.

[39] In accordance with this general shelf cooling and freshening, neutral density decreased over the 50 year period (Figure 5c), most notably in the dense waters of the Ross Sea ($\Delta\gamma^n = -0.0063 \pm 0.0097\ kg\ m^{-3}\ yr^{-1}$). Negative density changes were also seen in Prydz Bay ($\Delta\gamma^n = -0.0022 \pm 0.0007\ kg\ m^{-3}\ yr^{-1}$), near the tip of the Antarctic Peninsula ($\Delta\gamma^n = -0.0013 \pm 0.005\ kg\ m^{-3}\ yr^{-1}$),

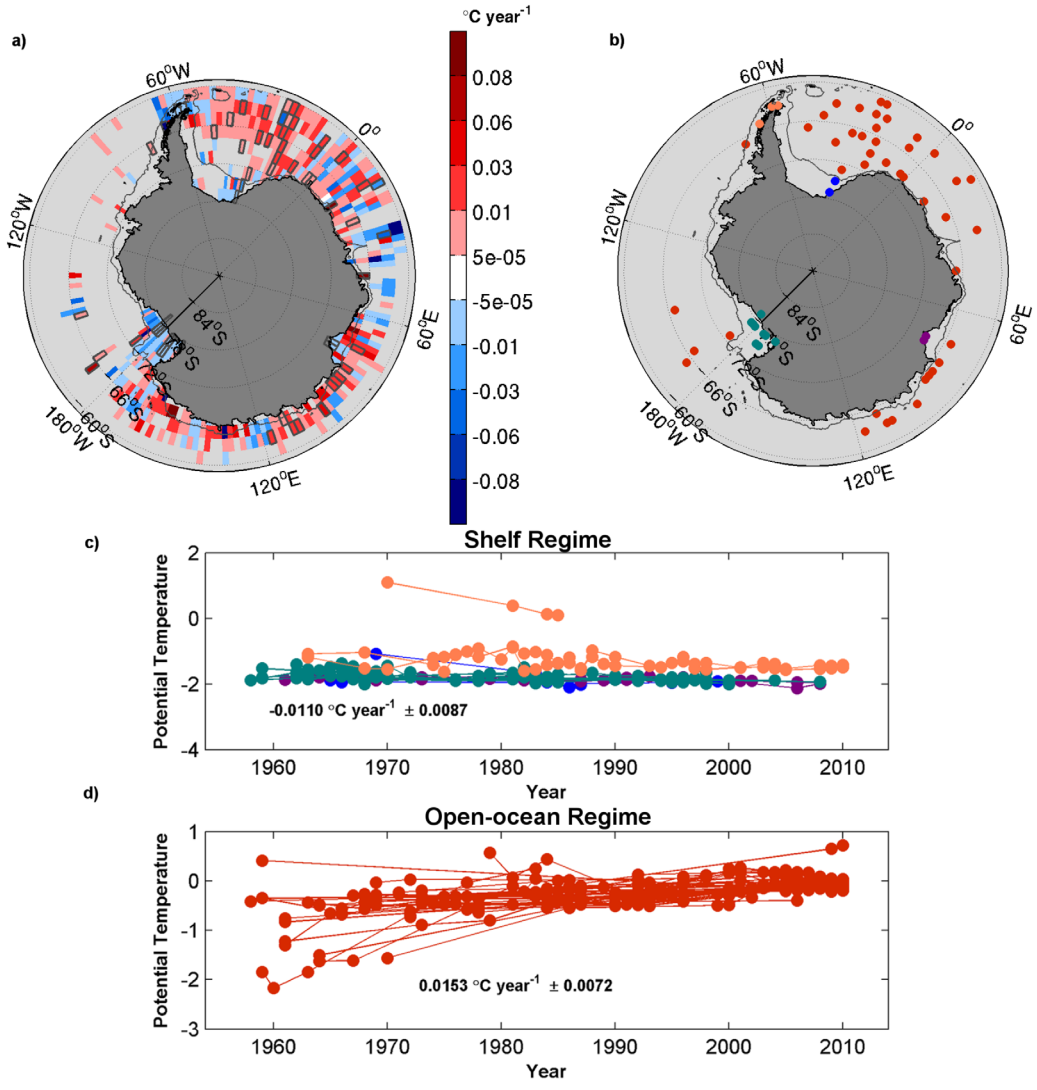

Figure 3. Potential temperature θ. (a) Time series trends within individual grid cells. The cells outlined in gray exhibit statistically significant linear trends. (b) Locations of the statistically significant trends. The colored dots correspond to the data shown in the lower two plots. (c) Statistically significant shelf-regime time series: green, Ross Sea; orange, Bransfield Strait and west of the Antarctic Peninsula; blue, southeastern Weddell Sea; and purple, Prydz Bay. (d) Statistically significant open ocean (AABW) time series (red). Mean linear rates of change and confidence intervals are also shown in Figures 3c and 3d.

and at the eastern edge of the Weddell Sea ($\Delta\gamma^n = -0.0006 \pm \text{inf kg m}^{-3}\text{ yr}^{-1}$). The average rate of γ^n change for all shelf regions combined was -0.0031 ± 0.0021 kg m^{-3} yr^{-1}.

[40] Figures 3d, 4d, and 5d show the statistically significant time series from the open ocean (AABW) regime. Statistically significant warming was seen most clearly in the Weddell, eastern Indian, and western Pacific sectors, where the historical data are relatively uniformly distributed. The overall mean temperature trend was positive: $+0.0153 \pm 0.0072$°C yr^{-1}. The salinity record was quite different, with statistically significant trends exhibiting no clear pattern of spatial distribution (Figure 4b) and, when averaged, indicating no overall salinity change ($\Delta S = 0.0000$ yr^{-1}; Figure 4d). Significant density decreases, on the other hand, were widely distributed (Figures 5a and 5b), with an overall rate of change of -0.0019 ± 0.0002 kg m^{-3} yr^{-1}; Figure 5d).

3.4. Comparisons Between Circum-Antarctic Anomaly Trends and Grid-Cell Property Trends

[41] Circum-Antarctic anomaly results provide estimates of general trends and processes acting in the Southern Ocean. In turn, results from the grid-cell property analysis shed a light on regional processes and presented themselves useful for a better comprehension of overall trends.

[42] The sensitivity of the circum-Antarctic shelf water temperature and open ocean salinity anomaly trends to the method of data handling (Figure 2 and Table 1) is possibly related to different physical processes acting within distinct regimes. While just one trend is shown by the whole-ocean time series, distinct variability patterns may arise for

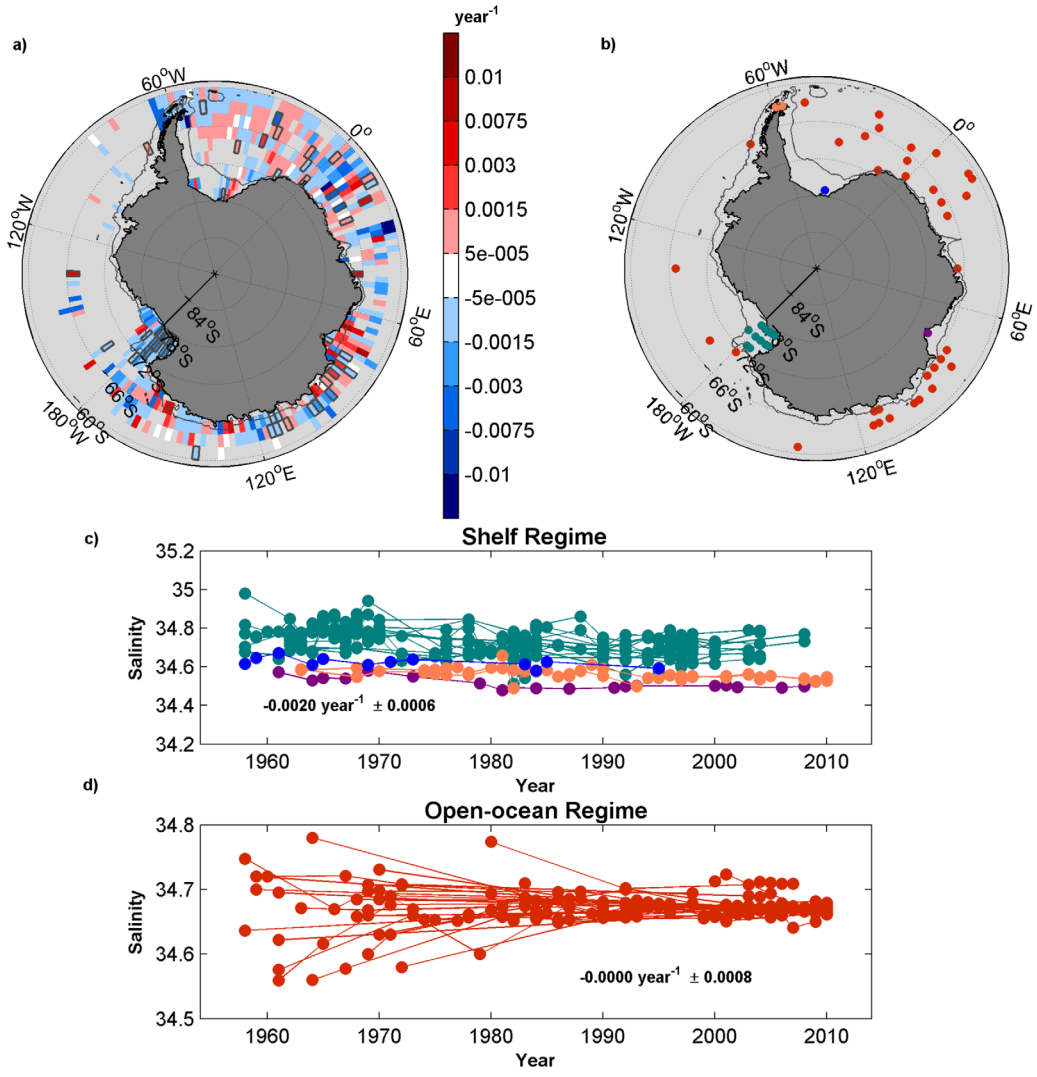

Figure 4. Same as Figure 3, but for salinity *S*.

different regions within the shelf and open ocean regimes. The use of filtered data and a spatially explicit approach (Figures 3–5) enable identification of spatially coherent patterns of variability and a better recognition of the dominant processes.

[43] The shelf water temperature change pattern was not clear on the circum-Antarctic anomaly trends due to the sensitivity of the trend sign to the choice of spatial binning method and also to the lack of statistical significance under any approach (Table 1). Examining spatially explicit trends and, moreover, limiting the evaluation to include only those grid cells with statistically significant temperature trends (Figures 3b and 3c) clarifies and confirms a cooling trend for all well-sampled shelf regions.

[44] Shelf freshening was clearly indicated in all analyses (Figures 2a and 4a–4c) and is identified together with cooling trends. Decreasing density was also consistently indicated under any methodology (Figures 2a and 5a–5c) and was likely a consequence of freshening not fully counterbalanced by cooling.

[45] For open ocean waters, warming was indicated in all of the analyses, with rates obtained using only the statistically significant grid-cell trends (Figure 3) being an order of magnitude higher than the circum-Antarctic anomaly trends (Figure 2 and Table 1). The lack of statistical significance in the freshening circum-Antarctic anomaly trends is consistent with the absence of a clear changing salinity pattern returned by the analysis of individual grid cells (Figures 4a and 4c–4d). Therefore, increasing temperature is likely the major factor driving the density changes shown in all methodologies (Figures 2b and 5b–5d).

[46] Although the different mechanisms responsible for the declining densities between dense Southern Ocean shelf and open ocean water masses, density decrease are evident for both regimes in all the methodologies assessed (Table 1 and Figures 2 and 5). For the open ocean regime, this decline is also evident in most of the sector-specific trends (Figure 1a). These factors suggest that the declining seawater density trend of dense Antarctic deep and bottom waters is widespread and highly consistent within the areas and time period covered by our data set. Based on a 2011 reoccupation of the Russia-US SO4P line from a 1992 WOCE cruise, *Swift and Orsi* [2012] reported AABW that was lighter by 0.06 kg m^{-3} due to a significant warming

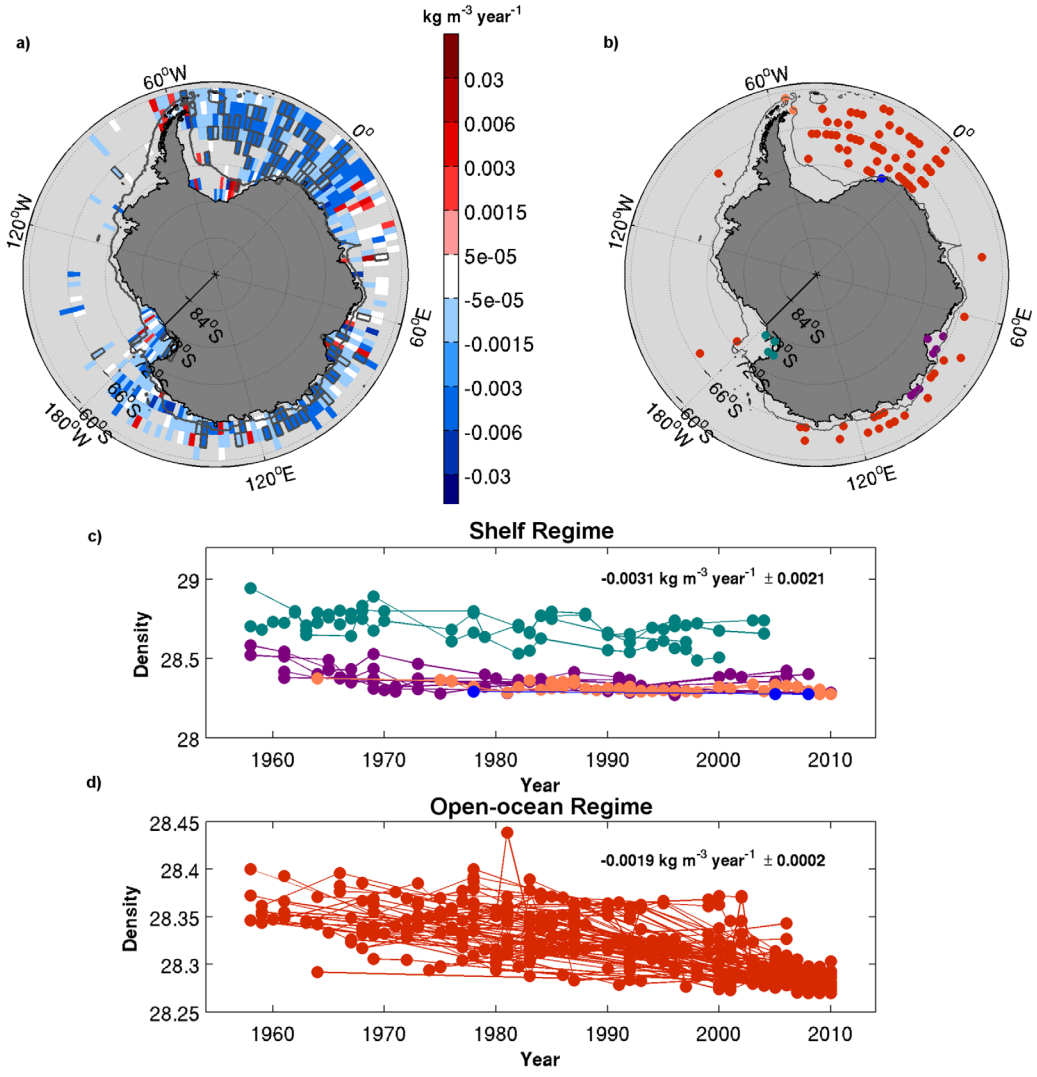

Figure 5. Same as Figure 3, but for neutral density γ^n.

($\Delta\theta = +0.1°C$) and a slight salinity reduction ($\Delta S = -0.04$) at the western boundary of the Ross Sea. Moreover, the bulk outflow of the newly formed Ross Sea Bottom Water was lighter and fresher than its threshold, and the thickness of the exported AABW layer had decreased. Our circumpolar results are in good agreement with the *Swift and Orsi* [2012] regional trends; both studies found fresher and lighter shelf/newly produced dense waters in addition to warmer and lighter open ocean dense waters.

[47] In most cases, the circum-Antarctic anomaly trends (Figure 2) presented the same variability patterns shown by the significant-only grid cell trends (Figures 3–5) but with lower values. This result is expected because the former approach considers all of the sampled Southern Ocean, including changing and unchanging regions, as a single entity, while the latter approach considers only those regions where property changes are most likely actually happening.

3.5. Decadal Changes in AABW Layer Volume

[48] AABW layer thickness through the decades is shown in Figure 6a. Overall, decadal thicknesses tended to be greatest in the Weddell basin, where values of 4000 m were attained. In the Indian sector, thicknesses ranged from 1000 to 3000 m. In the Western Pacific, average values were 1000–1500 m. These estimated AABW thicknesses are in agreement with the 2000–4000 m thickness described for the majority of the Southern Ocean [*Johnson*, 2008] based on WOCE Global Hydrographic Climatology. In 2008, the $\gamma^n = 28.27$ kg m^{-3} isopycnal at 60°S along the Greenwich Meridian was mapped at a depth of ~1500 m [see *Fahrbach et al.*, 2011, Figure 4d], which corresponds to a layer thickness of ~3500 m. Our estimate of layer thickness for the same location and time period ranges from 3500 to 4000 m.

[49] Decadal AABW volume anomalies (relative to the 1958–2010 average volume) are presented in Figure 6b. The period of 1978–1987 presented the largest positive anomalies. One contributing factor might be the possible enhancement of dense water production during the Weddell Polynya event of 1974–1976 [*Gordon*, 1978]. During the last two decades (1988–2010), negative volume anomalies clearly dominated the entire Southern Ocean.

[50] Total AABW volume reduction could not be determined due to sparse data coverage—i.e., the Southern

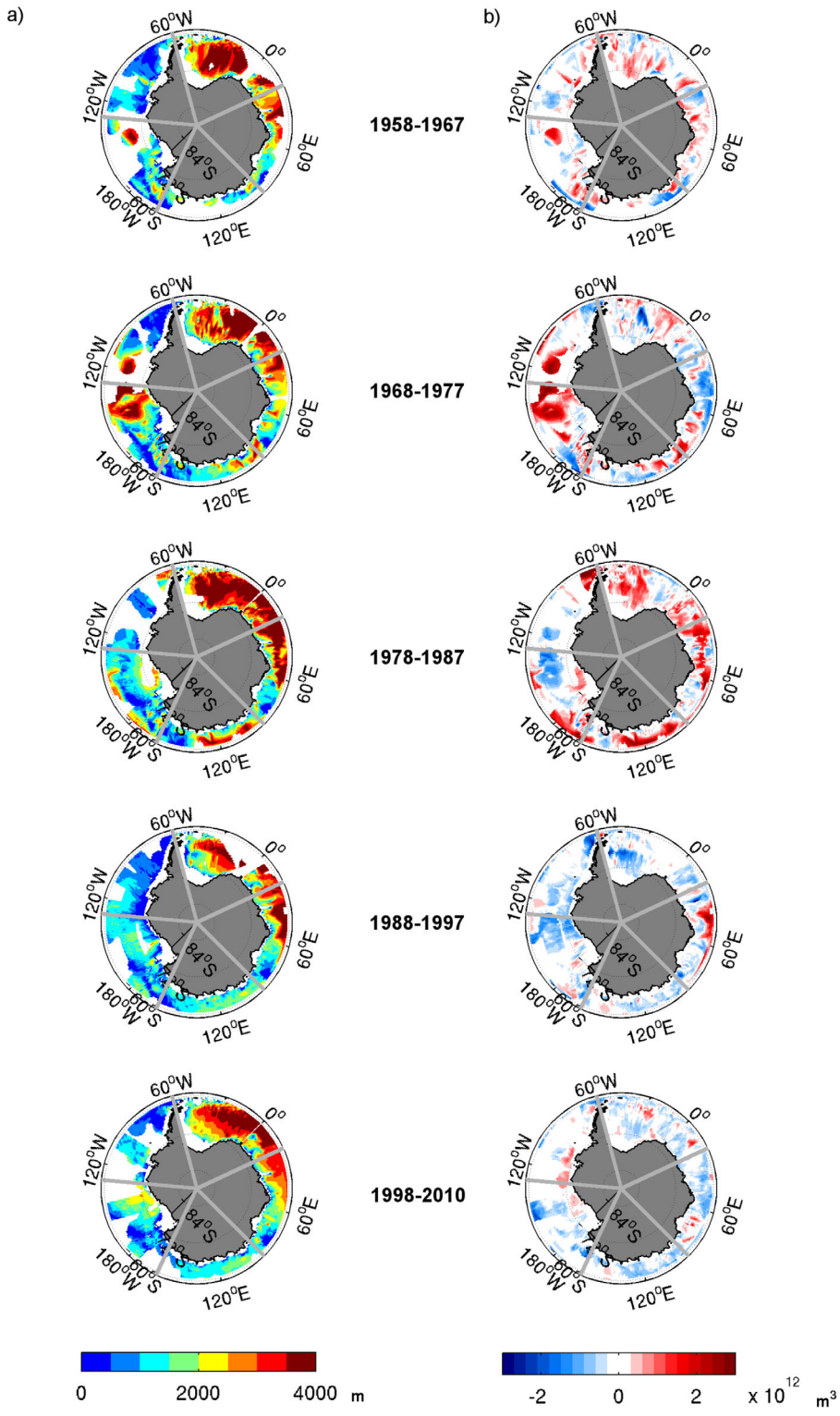

Figure 6. Decadal changes in Antarctic Bottom Water, 1958–2010. The radiating gray lines mark sector boundaries, as in Figure 1. (a) Decadal averages of AABW layer thickness (m). (b) AABW decadal volume anomalies (m^3) relative to the long-term (1958–2010) average.

Ocean basin was not completely covered in all decades by the fitted AABW upper surface. For the locations that were included, the average rate of change of AABW volume over the five decades was $-9.56 \times 10^{10} \pm 4.7 \times 10^9$ m^3 $decade^{-1}$, which is equivalent to an average upper-limit rate of change of -8.06 ± 0.38 m yr^{-1} for the period 1958–2010. Distinguishing among AABW varieties is beyond the scope of this paper, but we did perform the same estimation for the Weddell Sea Bottom Water isopycnal ($\gamma^n = 28.40$ kg m^{-3}) within the Weddell Sea sector.

This analysis resulted in a higher upper-limit rate of change (-13.05 ± 0.86 m yr^{-1}) than indicated for our AABW layer (which included both Weddell Sea Deep and Bottom Water in the Weddell Sea sector).

[51] A decrease of Southern Ocean AABW volume has been similarly reported for the period 1993–2006 [*Purkey and Johnson*, 2012]. For a bottom-water layer defined by $\theta \leq 0$°C (the isotherm equivalent of $\gamma^n \geq 28.27$ kg m^{-3} in the open ocean regime), a contraction rate of -8.2 ± 2.6 Sv was indicated. This estimate is based on the area-scaled sum of isotherm fall rates in the Australian-Antarctic (-13.2 ± 6.7 m yr^{-1}), Amundsen-Bellingshausen (-11.4 ± 2.9 m yr^{-1}), Weddell-Enderby (-8.1 ± 4.5 m yr^{-1}), Argentine (-9.5 ± 9.6 m yr^{-1}), and Agulhas-Mozambique (-6.4 ± 12.1 m yr^{-1}) basins and the Scotia Sea (-8.6 ± 40.3 m yr^{-1}). These fall rates (especially the Weddell-Enderby rate) are very similar to the average AABW upper-limit rate of change we estimated in this study. Our estimated average WSBW upper-limit rate of change is only half the WSBW descent rate estimated by *Purkey and Johnson* [2012] for the repeat section at the Prime Meridian (-22.5 ± 21.6 m yr^{-1}) but is comparable to their estimated rate for the inner Weddell Sea (-11.5 ± 13.4 m yr^{-1}).

3.6. Processes Contributing to Southern Ocean Temporal Trends

3.6.1. Shelf Water Hydrographic Trends

[52] Because Antarctic shelf water formation includes seawater interaction with ice shelves and sea ice, shelf waters are sensitive to some consequences of climate variability [e.g., *Huhn et al*., 2008]. Several factors could have contributed to the cooling and freshening trends observed in this study (Figures 2a, 3a–3c, and 4a–4c)—e.g., sea ice retreat, increased precipitation, enhanced melting of floating glacial ice, and increased melting of the Antarctic Ice Sheet [e.g., *Jacobs et al*., 2002; *Jacobs*, 2004; *Rintoul*, 2007; *Hellmer et al*., 2011]. These factors vary regionally.

[53] Freshening was observed in Bransfield Strait dense waters (Figures 4b and 4c), for which northwestern Weddell Sea shelf water has been commonly reported to be the main source [e.g., *Gordon and Nowlin*, 1978; *Whitworth et al*., 1994]. In the vicinity of Bransfield Strait, freshening has also been found on the shallow shelf around the tip of the Antarctic Peninsula ($\Delta S = -0.09$ for winter data, 1989–2006) [*Hellmer et al*., 2011]. Freezing-point shelf waters from the northwestern Weddell Sea shelf enter the strait from the region of Joinville Island, accounting for ~65% and ~90% of the mixture that constitutes eastern and central basin bottom water, respectively [*Gordon et al*., 2000]. Given the ice shelf mass loss events of the Antarctic Peninsula over the last 50 years [e.g., *Cook and Vaughan*, 2010], those shelf waters would be expected to carry a fresh and cold signal to Bransfield dense waters, consistent with the observed trends (Figures 3b–3c and 4b–4c). The Bransfield cyclonic recirculation identified by Lorena Luiz Collares et al. (manuscript in preparation, 2013) and corroborated by *Palmer et al*. [2012] may carry northwestern Weddell Sea signals into the strait region. However, a strong sea ice signal would be necessary to induce such changes in shelf water properties. In addition to these mass loss events, other factors such as increased precipitation and surface runoff could have contributed to shelf water cooling and freshening [*Hellmer et al*., 2011]. Bransfield Strait freshening ($\Delta S = -0.0014$ yr^{-1}) has been previously reported for central basin waters deeper than 1000 m and colder than -1.4°C [*Garcia and Mata*, 2005]. Because dense waters in the Bransfield Strait deep basins are reasonably isolated from adjacent waters by bathymetric features [*Wilson et al*., 1999], they are capable of preserving signals advected in from the northwestern Weddell Sea shelf region.

[54] Cooling and especially freshening in the Ross Sea shelf region have been widely documented [e.g., *Jacobs et al*., 2002; *Assmann and Timmermann*, 2005; *Jacobs*, 2006] and are clearly evident in our results (Figures 3a–3c and 4a–4c). A long-term examination of variability on the Ross Sea shelf indicated a freshening of High Salinity Shelf Water (HSSW; $\Delta S = -0.003$ yr^{-1}, 1958–2008) [*Jacobs and Giulivi*, 2010]. The same salinity trend was reported for the period 1963–2000 [*Jacobs et al*., 2002].

[55] The cooling we found for Ross Sea shelf dense waters ($\Delta\theta = -0.0045$°C yr^{-1}) is not entirely in accord with a previously reported slightly positive temperature trend ($\Delta\theta = \sim +0.0002$°C yr^{-1}, 1958–2008; *Jacobs and Giulivi*, 2010) associated with a rise in sea surface freezing point due to declining salinity. However, the temperature decrease evident in our data set could be seen as a recent signal. *Jacobs and Giulivi* [2010] showed that Modified Circumpolar Deep Water (MCDW) temperature and salinity near the Ross Ice Shelf decreased during the period 1967–2007 ($\Delta\theta \approx -0.0125$°C yr^{-1} and $\Delta S \approx -0.004$ yr^{-1}). MCDW is a subsurface water mass that results from mixing of slope-front current, deep, and shelf waters near the shelf break. Considering that recent CDW cooling is unlikely [e.g., *Gille*, 2002], local MCDW cooling is possibly a consequence of changes in shelf water properties, which reinforces the idea of local shelf water cooling. Another possibility to this process could be a change in shelf water contributions to the final MCDW mixture.

[56] Several factors, such as changes in precipitation, sea ice production, and ocean circulation strength, could have contributed to the cooling and freshening trends observed in the Ross Sea shelf region. Oxygen isotope data indicate that continental ice melt in the region of the West Antarctic Ice Sheet is likely the major contributor [*Jacobs et al*., 2002]. *Jacobs and Giulivi* [2010] and *Assmann and Timmermann* [2005] also identified the Amundsen Sea (into which about a third of the West Antarctic Ice Sheet drains; *Smith et al*. [2011]), as a source of Ross Sea shelf water *S* variability. Between 1991 and 2001, the West Antarctic Ice Sheet lost 154 ± 16 km^3 of ice to the ocean [*Shepherd et al*., 2002]. In the two decades following 1973, sea ice extent in the Bellingshausen/Amundsen Sea sector decreased by 20%, in correlation with an increase in west Antarctic surface air temperature [*Jacobs and Comiso*, 1997]. More recently (2003–2008), considerable thinning of the major Antarctic ice shelves has occurred. The most widespread and rapid losses occurred in West Antarctica, where thick ice shelves floating over deep troughs (e.g., the Amundsen Sea coast) enable fluctuating incursions of Circumpolar Deep Water beneath the ice shelves, thus leading to basal melting [*Pritchard et al*., 2012].

[57] These events—continental ice melt, sea ice changes, and ice shelf melting—seem to be related to the Southern

Annular Mode (SAM) positive phase. During positive phases, as occurred during the mid-1960s to 2000 [*Marshall*, 2003], strengthening of westerly winds can intensify the Antarctic Circumpolar Current [e.g., *Meredith et al*., 2004]. Consequences may include more intense CDW upwelling near the continental margin and enhanced CDW access to the shelf break [*Jacobs*, 2006], leading to greater heat supply to the sub-ice shelf cavities and increase in ice shelf basal melting [*Jacobs*, 2006; *Pritchard et al*., 2012].

[58] West Antarctic meltwater input events would generate Bellingshausen/Amundsen negative temperature and salinity anomalies, which would be transported westward by the Antarctic Slope Current to the Ross Sea. Mixing of this anomalous water with deep and shelf waters in the Ross Sea would affect HSSW and MCDW properties and, consequently, dense water mass formation [*Jacobs and Giulivi*, 2010]. Sparse sampling of the Bellingshausen/Amundsen Sea and open ocean Ross Sea regions prevents regional observational analysis and limits our understanding of the connections between the two areas.

3.6.2. Open Ocean (AABW) Hydrographic Trends

[59] Antarctic Bottom Water production results from the mixing of near-freezing-point shelf waters (HSSW and Ice Shelf Water, ISW) with relatively warm and salty intermediate waters (WDW, modified WDW, Circumpolar Deep Water, and MCDW). The source waters' hydrographic properties determine the characteristics of the recently formed AABW found over the continental slope and in the deep ocean. HSSW is formed by brine rejection during sea ice production, while ISW results from HSSW flowing in beneath ice shelves and mixing with glacial meltwater. Very few ISW measurements are available. The contribution of this water mass to AABW variability is therefore difficult to determine but may be important.

[60] Our analysis indicates that AABW generally warmed over the last half of the twentieth century, in contrast to the shelf waters, which generally cooled. Because Warm Deep Water constitutes the majority source water for AABW formation (62.5% WDW, 25.0% shelf water, and 12.5% Winter Water; *Foster and Carmack* [1976]), the WDW warming reported by *Fahrbach et al*. [2004] for the years 1992–1998 and by *Robertson et al*. [2002] for the 1970s–1990s could have driven the changes we found in deep and bottom waters (Figures 2a, 3a, and 3d).

[61] WDW warming inside the Weddell gyre could result from changes in external factors (e.g., a warmer or greater Circumpolar Deep Water inflow) or from changes in cooling processes within the Weddell Sea. The SAM-positive phase can influence both processes by shifting the Weddell front, thereby affecting Circumpolar Deep Water inflow and also increasing the gyre strength. This velocity increase would reduce the residence time of water inside the gyre, thereby reducing cooling during gyre advection [*Fahrbach et al*., 2004; *Robertson et al*., 2002]. Also, enhanced continental margin WDW upwelling during the positive phase would lead to a greater WDW contribution to high-density water formation [e.g., *Jacobs*, 2006; *Jullion et al*., 2010]. An increase in WDW contribution to the deep-ocean mixture in the WOCE SR4 and A12 sections, spanning 1984–1998, was shown by *Kerr et al*. [2009].

[62] Our analysis found no strong evidence for AABW freshening over the period of study. Several scenarios could explain the absence of a clear salinity trend. It is possible that the observed shelf freshening occurred recently enough that the signal had not, as of 2010, propagated widely throughout the open ocean. Shelf water residence times are ~4 and ~6 years for the Ross and Weddell Seas, respectively [*Trumbore et al*., 1991; *Schlosser et al*., 1991; *Mensch et al*., 1998]. The combination of shelf residence times plus transit times within the deep basins could account for a time lag between shelf freshening and widespread AABW freshening. (Warming, in contrast, probably occurs after AABW formation, within the deep basins.)

[63] It is also possible that shelf-driven freshening of open ocean waters is occurring but is being masked by other factors such as circulation, mixing, and residence times inside the deep basins. For example, a reduction in AABW production rate could lead to a longer residence period for deep and bottom waters within the deep ocean basins. More sluggish circulation could in turn contribute to the AABW warming through more prolonged mixing with relatively warmer and saltier surrounding waters [*Purkey and Johnson*, 2012]. This process could warm AABW, but disguise the freshening signal.

[64] The lack of a clear freshening trend in the Southern Ocean deep basins does not preclude the possibility that some portion of exported AABW is carrying a freshening signal to regions beyond AABW source areas. The densest bottom water formed in the Weddell Sea southern region enters the cyclonic gyre and recirculates within it, taking an indirect route to the Atlantic Ocean. At shallower depths, lower-salinity bottom water recently ventilated at the tip of the Antarctic Peninsula takes a more direct route [*Franco et al*., 2007] and is the first variety to be exported along the eastward flow of the northern Weddell Sea [*Gordon et al*., 2001]. This more direct path from the formation area to the deep basins of the global ocean entails a short AABW residence time within the Weddell Sea [*Fahrbach et al*., 1995]. Therefore, the shelf freshening signal could be carried out of the Weddell Sea by directly exported deep water [*Jullion et al.,* 2013] while being disguised within the gyre through mixing with saltier WDW. Observations of a decadal warming trend and a slight freshening of AABW flowing through the Vema Channel (~31°S, 39°W, 1991–2006) [*Zenk and Morozov*, 2007] may suggest possible propagation of a reduced salinity signal out of the Southern Ocean. An increase in WDW contributions to AABW formation could also serve to mask a freshening signal.

[65] All of these factors could have contributed to the observed range of regional AABW freshening trends, with no clear overall pattern (Figures 4b and 4d). For instance, freshening was seen in the vicinity of the shelf break between 90°E and 120°E, in the Australian-Antarctic Basin. This salinity decrease occurred in the same region where significant warming trends were observed (Figures 3b–3c). Australian-Antarctic basin freshening and warming, as well as reduced salinity in Ross Sea continental shelf waters, are in agreement with the results of *Shimada et al*. [2011]. They reported warming ($\Delta\theta = +0.004$°C yr^{-1}) and freshening ($\Delta S = -0.00026$ yr^{-1}) during the 1990s and 2000s in the Australian-Antarctic basin AABW layer denser than 28.30 kg m^{-3}.

[66] The observed changes in AABW neutral density reflect changes in both potential temperature and salinity

over the half-century examined. For the Antarctic shelf regions, the effects of freshening on density were not fully counterbalanced by the effects of cooling. Lower-density shelf waters resulted. For open ocean waters, however, warming seems to have been the major contributor to declining density. Production of a lighter dense water variety on the shelves (Figure 5c) could have contributed to the density decrease observed in both shelf and open ocean areas (Figures 2 and 5). In this case, it would be expected that not only the density decrease but also the freshening signal of the dense shelf waters (Figures 2a, 4c, and 5c) would be carried to the AABW water confined in the Southern Ocean deep basins. At present, however, the freshening trend seen in the shelf waters (Figures 4a–4c) is not clearly identifiable in the AABW layer (Figures 4a, 4b, and 4d). As noted above, this phenomenon could be the result of a shelf freshening signal that is not yet widespread or perhaps due to masking of a deep freshening signal by other processes.

3.6.3. AABW Volume Decrease

[67] The observed decrease in AABW volume (Figure 6b) could result from a number of factors—e.g., a reduced formation rate or changes in the properties of the dense water produced. Because our definition of AABW is based on a density threshold, the production of deep waters lighter than this defining limit, even at an unabated rate, would result in a volume decrease.

[68] Based on an examination of rates of volume change below potential isotherms within some of the world's deep basins, *Purkey and Johnson* [2012] quantified a global-scale contraction of AABW and concluded that the main cause was a slowdown of formation rate rather than changes in hydrographic properties. However, in light of our findings, we cannot reject the possibility that lighter deep and bottom waters may have been produced in recent years. It seems plausible that fresher and less-dense shelf waters (Figures 2a, 4c, and 5c) could have contributed to the production of lighter deep and bottom waters that warm after leaving the formation region, likely through mixing with warmer overlying waters during descent down the continental slope or within the deep basins. Both processes—freshening and post-production warming—could contribute to a decrease in AABW volume.

[69] Freshening-driven shelf water density reductions (Figures 2 and 5) could also hamper the sinking of dense water plumes to the ocean abyss [*Carmack and Killworth*, 1978]. This process would slow the AABW production and hence the bottom limb of the MOC [*Stouffer et al*., 2007], consistent with the reduced dense water production rate reported by *Purkey and Johnson* [2012]. A slower production rate would contribute to not only AABW volume reduction but also warming caused by a longer period of mixing with surrounding waters within the deep basins, as discussed above. The lack of information regarding ISW, a source water for WSBW, also leaves open the possibility that a weaker ISW contribution could result in changes in WSBW (and consequently AABW) properties and volume.

[70] In summary, we believe that production of lighter deep waters due to shelf water freshening is an important factor leading to a smaller AABW volume and the export of lighter water masses to the world ocean. Reduction of AABW formation rates, warming within deep ocean basins, and changing ISW contributions could also be involved.

4. Summary and Conclusions

[71] We used hydrographic data spanning 1958–2010 to investigate temporal changes in the potential temperature θ, salinity S, and neutral density γ^n of Southern Ocean shelf and open ocean dense waters (i.e., waters of $\gamma^n \geq 28.27$ kg m^{-3}). Some important geographic regions are practically devoid of the in situ data needed to assess long-term dense water mass variability. The Bellingshausen/Amundsen Seas sector is especially notable in this regard. Analytical strategies must therefore be carefully chosen to avoid misleading results and interpretations. Despite these data-coverage limitations, several important circumpolar trends are evident.

[72] Consideration of the entire Southern Ocean shelf regime as a single entity indicates a 50 year cooling trend that is not statistically significant. Spatially binning the data into 2° grid cells presents a clearer picture of shelf cooling in areas that have better data coverage, i.e., Bransfield Strait, Ross Sea, and Prydz Bay. These regions, important contributors to recently formed AABW, also clearly freshened and experienced declines in seawater density. These shelf salinity and density trends are robust regardless of the method used for spatial averaging.

[73] For the open ocean (AABW) regime as a whole, warming is indicated, but the statistical significance of this trend is sensitive to the method of spatial binning. Regional analysis indicates warming in most geographic sectors. Evidence for warming is most clear when time series trends are evaluated locally, within 2° grid cells. With this approach, AABW warming is seen over most of the open ocean regime, especially in the Weddell Sea, Indian, and Western Pacific Ocean sectors. For salinity, a single linear fit of all open ocean data yields a nonsignificant freshening trend, and evaluation of trends within individual grid cells indicates no coherent pattern of salinity change. Declining water density is indicated for most of the regional time series and is clearly evident in the grid-cell results regardless of the method used for geographic averaging.

[74] Our findings suggest that two important physical processes are occurring in the dense water masses of the Southern Ocean: (1) shelf freshening, which has resulted in decreasing density and (2) open ocean AABW warming that occurs after the water masses have left their formation regions. The shelf patterns, which are consistent with earlier reports from several regions (e.g., Bransfield Strait, Ross Sea, and Adelie Land), are probably caused by ice-ocean interactions. AABW warming could perhaps be caused by enhanced WDW contributions to AABW formation or by AABW mixing with recently warmed surrounding waters (e.g., WDW) during recirculation within the deep basins. Changes in ISW contributions to WSBW formation (presently poorly sampled and characterized) could also play a role. The SAM positive phase of the late twentieth century could have contributed to the observed AABW changes both directly and indirectly, by impacting melting rates and by increasing WDW temperatures and contributions to dense water formation.

[75] Seawater densities declined as a result of the θ and S changes, with density change rates of -0.0014 ± 0.0007 kg m^{-3} yr^{-1} for dense shelf waters and -0.0005 ± 0.0002 kg m^{-3} yr^{-1} for AABW. Limiting the analysis to those areas (grid cells) where the evidence is strongest (i.e., statistically significant) yields faster rates of change: -0.0031 ± 0.0021 kg m^{-3} yr^{-1} for shelf waters and -0.0019 ± 0.0002 kg m^{-3} yr^{-1} for AABW. Antarctic Bottom Water varieties exported from the Southern Ocean became significantly lighter during the five decades studied.

[76] Over the last two decades of the analysis, AABW volume decreased. Consideration of both shelf and open ocean trends suggests that the main causes were likely the production of lighter deep waters, a possible reduction in AABW formation rates, and AABW deep-basin warming.

[77] The widespread circumpolar trend of decreasing AABW found in this study could have implications beyond the Antarctic. If a constant AABW-layer density change of -0.0019 kg m^{-3} yr^{-1} (Figure 5d) is projected into the future, then AABW exported from the Southern Ocean would become as light as its source WDW (28.01 kg m^{-3}) in <150 years. Such a change could contribute to a slowing of the bottom branch of meridional overturning circulation, which could in turn impact global ocean circulation, marine ecosystems, sea level, ocean CO_2 storage, and global climate [e.g., *Rahmstorf*, 2006]. The extent of density change needed to alter ocean circulation is not well constrained.

[78] This study is the first to examine core hydrographic properties in all Antarctic marginal seas over an extended observational period, thus providing a more comprehensive view of long-term change, its probable causes, and possible consequences for the world ocean abyss. Our findings are consistent with those of earlier reports of warming and freshening from smaller-scale and shorter-term studies. Our work also illustrates that a trend analysis of hydrographic data must be conducted with care, especially for data-sparse regions such as the inhospitable but rapidly changing high-latitude oceans.

[79] Increased Southern Ocean sampling and modeling are needed for a better understanding of long-term hydrographic variability. To further elucidate the causes of recent changes in AABW hydrographic properties in deep ocean basins—e.g., changes in production rates, properties in formation areas, and export rates—a sampling strategy focused on key process-related features such as the continental shelf break would be especially beneficial. Filling in spatial data gaps (e.g., the Bellingshausen/Amundsen Seas and Ross Sea sectors) will continue to be important as well.

[80] **Acknowledgments.** This study is a contribution to the International Polar Year SOS-CLIMATE project through the activities of the Brazilian High Latitudes Oceanography Group (GOAL) in the Brazilian Antarctic Program (PROANTAR). GOAL has been funded by the Brazilian Ministry of the Environment (MMA); the Brazilian Ministry of Science, Technology and Innovation (MCTI); and the Council for Research and Scientific Development of Brazil (CNPq; 550370/2002-1; 520189/2006-0). The authors thank the Brazilian National Institute of Science and Technology of Cryosphere (INCT-CRIOSFERA; 573720/2008-8) and the POLARCANION project (CNPq 556848/2009-8). M.A. and R.K. acknowledge financial support received from the CAPES Foundation and FAPERGS. We also thank the crew of the Brazilian Navy research ship *Ary Rongel* for their assistance during the field sampling of the GOAL cruises. We would like to acknowledge Hartmut H. Hellmer and the anonymous reviewers for their constructive comments, which greatly improved the manuscript.

References

Aoki, S., S. Rintoul, S. Ushio, and S. Watanabe (2005), Freshening of the Adelie Land Bottom Water near 140°E, *Geophys. Res. Lett.*, *32*, L23601, doi:2007GL030340/2005GL024246.

Assmann, K. M., and R. Timmermann (2005), Variability of dense water formation in the Ross Sea, *Ocean Dyn.*, *55*(2), 68–87, doi:10.1007/s10236-004-0106-7.

Boyer, T. P., S. Levitus, and J. I. Antonov (2005), Linear trends in salinity for the World Ocean, 1955–1998, *Geophys. Res. Lett.*, *32*, L01604, doi:2007GL030340/2004GL021791.

Boyer, T. P., et al. (2009), *World Ocean Database 2009, NOAA Atlas NESDIS*, vol. *66*, edited by S. Levitus, DVD, U.S. Gov. Print. Off., Washington, D. C.

Broecker, W. S., et al. (1998), How much deep water is formed in the Southern Ocean?, *J. Geophys. Res.*, *103*, 15,833–15,843.

Carmack, E. C., and T. D. Foster (1975), On the flow of water out of the Weddell Sea, *Deep Sea Res. Oceanogr. Abstr.*, *22*, 711–724.

Carmack, E. C., and P. D. Killworth (1978), Formation and interleaving of abyssal water masses off Wilkes Land, Antarctica, *Deep Sea Res.*, *25*, 357–369.

Cavalieri, D. J., and C. L. Parkinson (2008), Antarctic sea ice variability and trends, 1979–2006, *J. Geophys. Res.*, *113*, C07004, doi:2007GL030340/2007JC004564.

Cook, A. J., and D. G. Vaughan (2010), Overview of areal changes of the ice shelves on the Antarctic Peninsula over the past 50 years, *Cryosphere*, *4*(1), 77–98, doi:10.5194/tc-4-77-2010.

Fahrbach, E., G. Rohardt, N. Scheele, N. Schroder, V. Strass, and A. Wisotzki (1995), Formation and discharge of deep and bottom water in the northwestern Weddell Sea, *J. Mar. Res.*, *53*, 515–538.

Fahrbach, E., M. Hoppema, G. Rohardt, M. Schröder, and A. Wisotzki (2004), Decadal-scale variations of water mass properties in the deep Weddell Sea, *Ocean Dyn.*, *54*, 77–91.

Fahrbach, E., M. Hoppema, G. Rohardt, O. Boebel, O. Klatt, and A. Wisotzki (2011), Warming of deep and abyssal water masses along the Greenwich meridian on decadal time scales: The Weddell gyre as a heat buffer, *Deep Sea Res., Part II*, *58*(25–26), 2509–2523, doi:10.1016/j.dsr2.2011.06.007.

Franco, B., M. M. Mata, A. R. Piola, and C. A. E. Garcia (2007), Northwestern Weddell Sea deep outflow into the Scotia Sea during the austral summers of 2000 and 2001 estimated by inverse methods, *Deep Sea Res., Part I*, *54*, 1815–1840.

Fofonoff, N. P. (1956), Some properties of sea water influencing the formation of Antarctic Bottom Water, *Deep Sea Res.*, *4*, 32–35.

Foster, T. D., and E. C. Carmack (1976), Frontal zone mixing and Antarctic Bottom Water formation in the southern Weddell Sea, *Deep Sea Res. Oceanogr. Abstr.*, *23*, 301–317.

Garcia, C. A. E., and M. M. Mata (2005), Deep and bottom water variability in the central basin of Bransfield Strait (Antarctica) over the 1980–2005 period, *CLIVAR Exch.*, *10*(4), 48–50.

Gille, S. T. (2002), Warming of the Southern Ocean since the 1950s, *Science*, *295*, 1275–1277.

Gille, S. T. (2008), Decadal-scale temperature trends in the Southern Hemisphere Ocean, *J. Clim.*, *21*(18), 4749–4765, doi:10.1175/2008JCLI2131.1.

Gordon, A. L. (1978), Deep antarctic convection west of maud rise. *J. Phys. Oceanogr., 8*, 600–612.

Gordon, A. L., and W. D. Nowlin Jr. (1978), The basin waters of the Bransfield Strait, *J. Phys. Oceanogr.*, *8*, 258–264.

Gordon, A. L., M. Mensch, D. Zhaoqian, W. M. Smethie, and J. de Bettencourt (2000), Deep and bottom water of the Bransfield Strait eastern and central basins, *J. Geophys. Res.*, *105*, 11,337–11,346, doi:2007GL030340/2000JC900030.

Gordon, A. L., M. Visbeck, and B. Huber (2001), Export of Weddell Sea deep and bottom water, *J. Geophys. Res.*, *106*, 9005–9017, doi:2007GL030340/2000JC000281.

Hellmer, H. H., O. Huhn, D. Gomis, and R. Timmermann (2011), On the freshening of the northwestern Weddell Sea continental shelf, *Ocean Sci.*, *7*, 305–316, doi:10.5194/os-7-305-2011.

Huhn, O., H. H. Hellmer, M. Rhein, C. Rodehacke, W. Roether, M. P. Schodlok, and M. Schröder (2008), Evidence of deep-and bottom-water

formation in the western Weddell Sea, *Deep Sea Res., Part II*, *55*, 1098–1116.

Jackett, D. R., and T. J. McDougall (1997), A neutral density variable for the world's ocean, *J. Phys. Oceanogr.*, *27*(2), 237–263.

Jacobs, S. S. (2004), Bottom water production and its links with the thermohaline circulation, *Antarct. Sci.*, *16*(4), 427–437, doi:10.1017/S095410200400224X.

Jacobs, S. (2006), Observations of change in the Southern Ocean, *Philos. Trans. R. Soc. A*, *364*, 1657–1681.

Jacobs, S. S., and J. C. Comiso (1997), Climate variability in the Amundsen and Bellingshausen Seas, *J. Clim.*, *10*, 697–709.

Jacobs, S. S., and C. F. Giulivi (2010), Large multidecadal salinity trends near the Pacific–Antarctic continental margin, *J. Clim.*, *23*, 4508–4524, doi:10.1175/2010JCLI3284.1.

Jacobs, S. S., C. F. Giulivi, and P. A. Mele (2002), Freshening of the Ross Sea during the late 20th century, *Science*, *297*(386), doi:10.1126/science.1069574.

Johnson, G. C. (2008), Quantifying Antarctic Bottom Water and North Atlantic Deep Water volumes, *J. Geophys. Res.*, *113*, C05027, doi:2007GL030340/2007JC004477.

Johnson, G. C., S. G. Purkey, and J. L. Bullister (2008), Warming and freshening in the abyssal southeastern Indian Ocean, *J. Clim.*, *21*, 5351–5363.

Johnson, D. R., H. E. Garcia, and T. P. Boyer (2009),World Ocean Database 2009 Tutorial, *NODC Int. Rep. 21*, edited by S. Levitus, 18 pp., NOAA Print. Off., Silver Spring, Md. [Available at http://www.nodc.noaa.gov/OC5/WOD09/pr_wod09.html.]

Jullion, L., S. C. Jones, A. C. Naveira Garabato, and M. P. Meredith (2010), Wind-controlled export of Antarctic Bottom Water from the Weddell Sea, *Geophys. Res. Lett.*, *37*, L09609, doi:2007GL030340/2010GL042822.

Jullion, L., A. Naveira Garabato, M. Meredith, P. Holland, P. Courtois, and B. King (2013), Decadal freshening of the Antarctic Bottom Water exported from the Weddell Sea, *J. Clim.,* doi:10.1175/JCLI-D-12-00765.1, in press.

Kerr, R., M. M. Mata, and C. A. E. Garcia (2009), On the temporal variability of the Weddell Sea Deep Water Masses, *Antarct. Sci.*, *21*, 383–400, doi:10.1017/S0954102009001990.

Kerr, R., K. J. Heywood, M. M. Mata, and C. A. E. Garcia (2012), On the outflow of dense water from the Weddell and Ross Seas in OCCAM model, *Ocean Sci.*, *8*(3), 369–388, doi:10.5194/os-8–369-2012.

Lumpkin, R., and K. Speer (2007), Global ocean meridional overturning, *J. Phys. Oceanogr.*, *37*, 2550–2562.

Marshall, G. J. (2003), Trends in the Southern Annular Mode from observations and reanalyses, *J. Clim.*, *16*, 4134–4143.

Marshall, G. J., O. Andrew, P. M. L. Nicole, and J. C. King (2006), The impact of a changing Southern Hemisphere Annular Mode on Antarctic peninsula summer temperatures, *J. Clim.*, *19*, 5388–5404.

Mayewski, P. A., et al. (2009), State of the Antarctic and Southern Ocean climate system, *Rev. Geophys.*, *47*, RG1003, doi:2007GL030340/2007RG000231.

Mendes, C. R. B., M. S. Souza, V. M. T. Garcia, M. C. Leal, V. Brotas, and C. A. E. Garcia (2012), Dynamics of phytoplankton communities during late summer around the tip of the Antarctic Peninsula, *Deep Sea Res., Part 1*, *65*, 1–14.

Mensch, M., A. Simom, and R. Bayer (1998), Tritium and CFC input functions for the Weddell Sea, *J. Geophys. Res.*, *103*, 15,923–15,937.

Meredith, M. P., and J. C. King (2005), Rapid climate change in the ocean west of the Antarctic Peninsula during the second half of the 20th century, *Geophys. Res. Lett.*, *32*, L19604, doi:2007GL030340/2005GL024042.

Meredith, M. P., P. L. Woodworth, C. W. Hughes, and V. Stepanov (2004), Changes in the ocean transport through Drake Passage during the 1980s and 1990s, forced by changes in the Southern Annular Mode, *Geophys. Res. Lett.*, *31*, L21305, doi:2007GL030340/2004GL021169.

Nicholls, K. W., S. Østerhus, K. Makinson, T. Gammelsrød, and E. Fahrbach (2009), Ice-ocean processes over the continental shelf of the southern Weddell Sea, Antarctica: A review, *Rev. Geophys.*, *47*, RG3003, doi:2007GL030340/2007RG000250.

Orsi, A. H., and C. L. Wiederwohl (2009), A recount of Ross Sea waters, *Deep Sea Res., Part II*, *56*, 778–779, doi:10.1016/j.dsr2.2008.10.033.

Orsi, A. H., G. C. Johnson, and J. L. Bullister (1999), Circulation, mixing and production of Antarctic Bottom Water, *Prog. Oceanogr.*, *43*, 55–109.

Palmer, M., D. Gomis, M. D. M. Flexas, G. Jordà, L. Jullion, T. Tsubouchi, and A. C. Naveira Garabato (2012), Water mass pathways and transports over the South Scotia Ridge west of 50°W, *Deep Sea Res., Part I*, *59*, 8–24, doi:10.1016/j.dsr.2011.10.005.

Pritchard, H. D., S. R. M. Ligtenberg, H. Fricker, D. G. Vaughan, M. R. van den Broeke, and L. Padman (2012), Antarctic ice-sheet loss driven by basal melting of ice shelves, *Nature*, *484*(7395), 502–505, doi:10.1038/nature10968.

Purkey, S. G., and G. C. Johnson (2010), Warming of global abyssal and deep Southern Ocean waters between the 1990s and 2000s: Contributions to global heat and sea level rise budgets, *J. Clim.*, *23*, 6336–6351.

Purkey, S. G., and G. C. Johnson (2012), Global contraction of Antarctic Bottom Water between the 1980s and 2000s, *J. Clim.*, *25*, 5830–5844, doi:10.1175/JCLI-D-11–00612.1.

Rahmstorf, S. (2006), Thermohaline ocean circulation, in *Encyclopedia of Quaternary Sciences*, edited by S. A. Elias, pp. 739–750, Elsevier, Amsterdam.

Rignot, E., G. Casassa, P. Gogineni, W. Krabill, A. Rivera, and R. Thomas (2004), Accelerated ice discharge from the Antarctic Peninsula following the collapse of Larsen B iceshelf, *Geophys. Res. Lett.*, *31*, L18401, doi:2007GL030340/2004GL020697.

Rintoul, S. R. (2007), Rapid freshening of Antarctic Bottom Water formed in the Indian and Pacific oceans, *Geophys. Res. Lett.*, *34*, L06606, doi:2007GL030340/2006GL028550.

Robertson, R., M. Visbeck, A. L. Gordon, and E. Fahrbach (2002), Long-term temperature trends in the deep waters of the Weddell Sea, *Deep Sea Res., Part II*, *49*(21), 4791–4806, doi:10.1016/S0967-0645(02)00159-5.

Schlosser, P., J. L. Bullister, and R. Bayer (1991), Studies of deep water formation and circulation in the Weddell Sea using natural and anthropogenic tracers, *Mar. Chem.*, *35*, 97–122.

Schmittner, A., J. C. H. Chiang, and S. R. Hemming (2007), Introduction: The ocean's meridional overturning circulation, in *Ocean Circulation: Mechanisms and Impacts*, Geophys. Monogr. Ser., *173*, p. 392, AGU, Washington, D. C.

Shepherd, A. P., D. J. Wingham, and J. A. D. Mansley (2002), Inland thinning of the Amundsen Sea sector, West Antarctica, *Geophys. Res. Lett.*, *29*(10), 1364, doi:2007GL030340/2001GL014183.

Shimada, K., S. Aoki, K. I. Ohshima, and S. R. Rintoul (2011), Influence of Ross Sea Bottom Water changes on the warming and freshening of the Antarctic Bottom Water in the Australian-Antarctic Basin, *Ocean Sci. Discuss.*, *8*, 2197–2235, doi:10.5194/osd-8–2197–2011.

Smith, J. A., C.-D. Hillenbrand, G. Kuhn, R. D. Larter, A. G. C. Graham, W. Ehrmann, S. G. Moreton, and M. Forwick (2011), Deglacial history of the West Antarctic Ice Sheet in the western Amundsen Sea Embayment, *Quat. Sci. Rev.*, *30*(5–6), 488–505, doi:10.1016/j.quascirev.2010.11.020.

Stouffer, R. J., D. Seidov, and B. J. Haupt (2007), Climate response to external sources of freshwater: North Atlantic versus the Southern Ocean, *J. Clim.*, *20*, 436–448, doi:10.1175/JCLI4015.1.

Swift, J. H., and A. H. Orsi (2012), Sixty-four days of hydrography and storms: RVIB Nathaniel B. Palmer's 2011 S04P Cruise, *Oceanography*, *25*(3), 54–55, doi:10.5670/oceanog.2012.74.

Trumbore, S. E., S. S. Jacobs, and W. M. Smethie Jr. (1991), Chlorofluorocarbon evidence for rapid ventilation of the Ross Sea, *Deep Sea Res., Part A*, *38*, 845–870.

Turner, J., S. R. Colwell, G. J. Marshall, T. A. Lachilan-Cope, A. M. Carleton, P. D. Jones, V. Lagun, P. A. Reid, and S. Iagovkina (2005), Antarctic climate change during the last 50 years, *Int. J. Climatol.*, *25*, 279–294.

Whitworth, T., W. Nowlin, A. Orsi, R. A. Locarnini, and S. G. Smith (1994), Weddell Sea shelf water in the Bransfield Strait and Weddell-Scotia confluence, *Deep Sea Res., Part I*, *41*(4), 629–641.

Whitworth, T., A. H. Orsi, S. J. Kim, W. D. Nowlin Jr., and R. A. Locarnini (1998), Water masses and mixing near the Antarctic slope front, in *Ocean, Ice, and Atmosphere: Interactions at the Antarctic Continental Margin, Antarct. Res. Ser.*, vol. *75*, edited by S. S. Jacobs and R. F. Weiss, pp. 1–27, AGU, Washington, D. C., doi:2007GL030340/AR075p0001.

Wilson, T., G. P. Klinkhammer, and C. S. Chin (1999), Hydrography within the Central and East Basins of the Bransfield Strait, Antarctica, *J. Phys. Oceanogr.*, *29*, 465–479.

Zenk, W., and E. Morozov (2007), Decadal warming of the coldest Antarctic Bottom Water flow through the Vema Channel, *Geophys. Res. Lett.*, *34*, L14607, doi:2007GL030340/2007GL030340.